The L6 Protein TM4SF1 Is Critical for Endothelial Cell Function and Tumor Angiogenesis

Shou-Ching Shih,[1] Andrew Zukauskas,[1] Dan Li,[1] Guanmei Liu,[1] Lay-Hong Ang,[2] Janice A. Nagy,[1] Lawrence F. Brown,[1] and Harold F. Dvorak[1]

[1]Center for Vascular Biological Research and Department of Pathology, and [2]Imaging Core Facility, Beth Israel Deaconess Medical Center, Harvard Medical School, Boston, Massachusetts

Abstract

Transmembrane-4-L-six-family-1 (TM4SF1) was originally described as a cancer cell protein. Here, we show that it is highly expressed in the vascular endothelium of human cancers and in a banded pattern in the filopodia of cultured endothelial cells (EC). TM4SF1 knockdown prevented filopodia formation, inhibited cell mobility, blocked cytokinesis, and rendered EC senescent. Integrin-α5 and integrin-β1 subunits gave a similar staining pattern and interacted constitutively with TM4SF1, whereas integrin subunits often associated with angiogenesis (αV, β3, β5) interacted with TM4SF1 only after vascular endothelial growth factor (VEGF)-A or thrombin stimulation. TM4SF1 knockdown substantially inhibited maturation of VEGF-A^{164}–induced angiogenesis. Thus, TM4SF1 is a key regulator of EC function *in vitro* and of pathologic angiogenesis *in vivo* and is potentially an attractive target for antiangiogenesis therapy. [Cancer Res 2009;69(8):3272–7]

Introduction

Transmembrane-4-L-six-family-1 (TM4SF1), also known as L6, was first identified as a protein abundantly expressed in a variety of epithelial cancer cells (1, 2) and weakly expressed in normal vascular endothelium (3, 4). It has the topology of a tetraspanin (5); however, TM4SF1 and five other structurally similar proteins (TM4SF4, 5, 18, 19, and 20) lack overall sequence homology with the 33 genuine tetraspanins, and the characteristic CCG motif in the large extracellular loop (5). Therefore, these proteins have been classified separately as the L6 family (5).

Experiments on tumor cells had previously shown TM4SF1 to be important for growth (1), motility (6), invasion (7), and metastasis (8). However, the role of TM4SF1 in vascular endothelium has not been investigated. We report here that TM4SF1 is overexpressed in the vascular endothelial cells (EC) of several human cancers and is critically important for their function.

Materials and Methods

Antibodies, soluble factors. Antibodies were as follows: mouse antihuman TM4SF1, ITGA5, ITGAV, ITGB1, ITGB3, and ITGB5 (Millipore); Cy3-conjugated mouse anti-human α-smooth muscle actin (αSMA; Sigma); goat anti-human VE-cadherin (Santa Cruz); FITC-labeled anti-mouse IgG; and Texas red–labeled rabbit anti–goat-IgG (Invitrogen). Vascular endothelial growth factor (VEGF)-A, basic fibroblast growth factor (bFGF), transforming growth factor β (TGFβ), hepatocyte growth factor (HGF), and tumor necrosis factor (TNF)α were from R&D Laboratories, and thrombin was from Calbiochem.

Mice, adenoviral vectors. Athymic nude mice were obtained from National Cancer Institute. All studies were performed under protocols approved by the Beth Israel Deaconess Medical Center Institutional Animal Care and Use Committee. Adenoviral vectors expressing mouse VEGF-A^{164} (Ad-VEGF-A^{164}) and Lac-Z (Ad-Lac-Z) were described previously (9–11).

Cells, flow cytometry, and immunostaining. Human umbilical vein Ecs (HUVEC) and other EC were from Clonetics. Cells were grown in growth medium-2-MV (Clonetics) and used at passage 5 to 6. For flow cytometry, EC were stained with propidium iodide and 10^4 events were collected for each experiment (Becton Dickinson). EC were grown on 8-mm cover glasses, fixed in 4% paraformaldehyde (5 min, 25°C), blocked with PBS/1% fetal bovine serum, and immunostained (12). Filamentous actin (F-actin) was visualized with rhodamine-conjugated phalloidin (Millipore). Crystal violet (50 mg/mL, 2 h, 25°C) and senescent Staining kit (Sigma) were from Sigma. Paraformaldehyde-fixed, paraffin-embedded tissue sections were stained with hematoxylin or were immunostained with TM4SF1 primary (1:300×) and secondary antibodies, saturated binding site with excess mouse IgG, and added costaining primary antibodies (13).

Gene silencing. Short hairpin RNA (shRNA)-expressing adenoviruses were generated using the BLOCK-iT Adenoviral-RNAi System (Invitrogen). Sequences of TM4SF1 shRNAs were as follows: human, GCACGATGCATCGGACATTCT and GCTATGGGAAGTGTGCACGAT; mouse, GCTATGAGCCCAAGCATATTG; control, GTACGTACGTACGTACGTACT. The pAd/BLOCK-iT/shRNA construct was transfected into 293A cells for adenovirus production. Adenoviruses were purified using the Adenopure kit (PureSyn). Virus titer was determined by multiplicity of infection (moi).

Multigene transcriptional profiling. Multigene transcriptional profiling is a quantitative real-time PCR technique that efficiently provides mRNA copies per cell (14). Total RNA was prepared using the RNeasy kit with DNase-I treatment (Qiagen) and cDNA using random primers and SuperScript III (Invitrogen). For each data point, mean ± SD were calculated from three samples from three separate experiments. PCR reactions for each cDNA sample were performed in duplicate. Transcript abundances were normalized per 10^6 18S-rRNA copies to approximate number of transcripts per cell (15, 16).

***In situ* hybridization.** *In situ* hybridization was performed as described (12). Tissues were fixed in 4% paraformaldehyde (PFA) and cryostat sections were hybridized overnight with antisense or sense (control) ^{35}S-labeled RNA probes specific for human TM4SF1 (NM014220.2, nt 1230–1630) or murine TM4SF1 (NM_008536.3, nt 643–1075).

Immunoprecipitation and Western blotting. HUVEC were lysed in TBS (pH 7.0), 1% Brij99, protease inhibitor cocktail (Sigma), and pretreated with mouse IgG before immunoprecipitation. Western blots were performed with a 1:500 dilution of primary antibodies and a 1:10,000 dilution of horseradish peroxidase–conjugated goat anti-mouse IgG (Millipore). Blots were developed with the ECL system (GE Healthcare).

Angiogenesis quantification. Evan's Blue dye was injected i.v. into nude mice anesthetized with Avertin (200 mg/kg; ref. 10). Five minutes later, after equilibration in blood but before significant plasma leakage, mice were

Note: Supplementary data for this article are available at Cancer Research Online (http://cancerres.aacrjournals.org/).

Requests for reprints: Shou-Ching Shih and Harold F. Dvorak, Pathology Department, Beth Israel Deaconess Medical Center, 99 Brookline Avenue, Boston, MA 02215. Phone: 617-667-8156/617-667-8529; Fax: 617-667-3591; E-mail: sshih2@bidmc.harvard.edu and hdvorak@bidmc.harvard.edu.

doi:10.1158/0008-5472.CAN-08-4886

euthanized and angiogenic sites were harvested with an 8-mm punch. Dye was extracted at 65°C for 48 h in 0.5 mL formamide. Triplicate 100 μL samples were measured at OD_{620} nm.

Statistical analysis. Statistics were performed with Student's *t* test.

Results and Discussion

TM4SF1 expression in human cancers. TM4SF1 was found to be highly expressed in the vascular endothelium of smooth muscle cell–coated blood vessels that supply several important human cancers, including those in which the malignant cells themselves did not express TM4SF1 detectably (Fig. 1*A* and *B*). The vasculature supplying nearby normal tissues expressed TM4SF1 weakly (data not shown), consistent with published observations (3).

TM4SF1 expression in cultured EC. TM4SF1 was expressed at consistently high levels (70–90 mRNA copies per cell) in several cultured EC, including umbilical vein (HUVEC), coronary artery (human coronary artery endothelial cell), pulmonary artery (human pulmonary artery endothelial cell), dermal microvascular (human dermal microvascular endothelial cell), and lymphatic (human lymphatic endothelial cell; Fig. 1*C, left*). In contrast, TM4SF1 expression was low (<5 mRNA copies per cell) in human dermal fibroblasts and smooth muscle cells (data not shown).

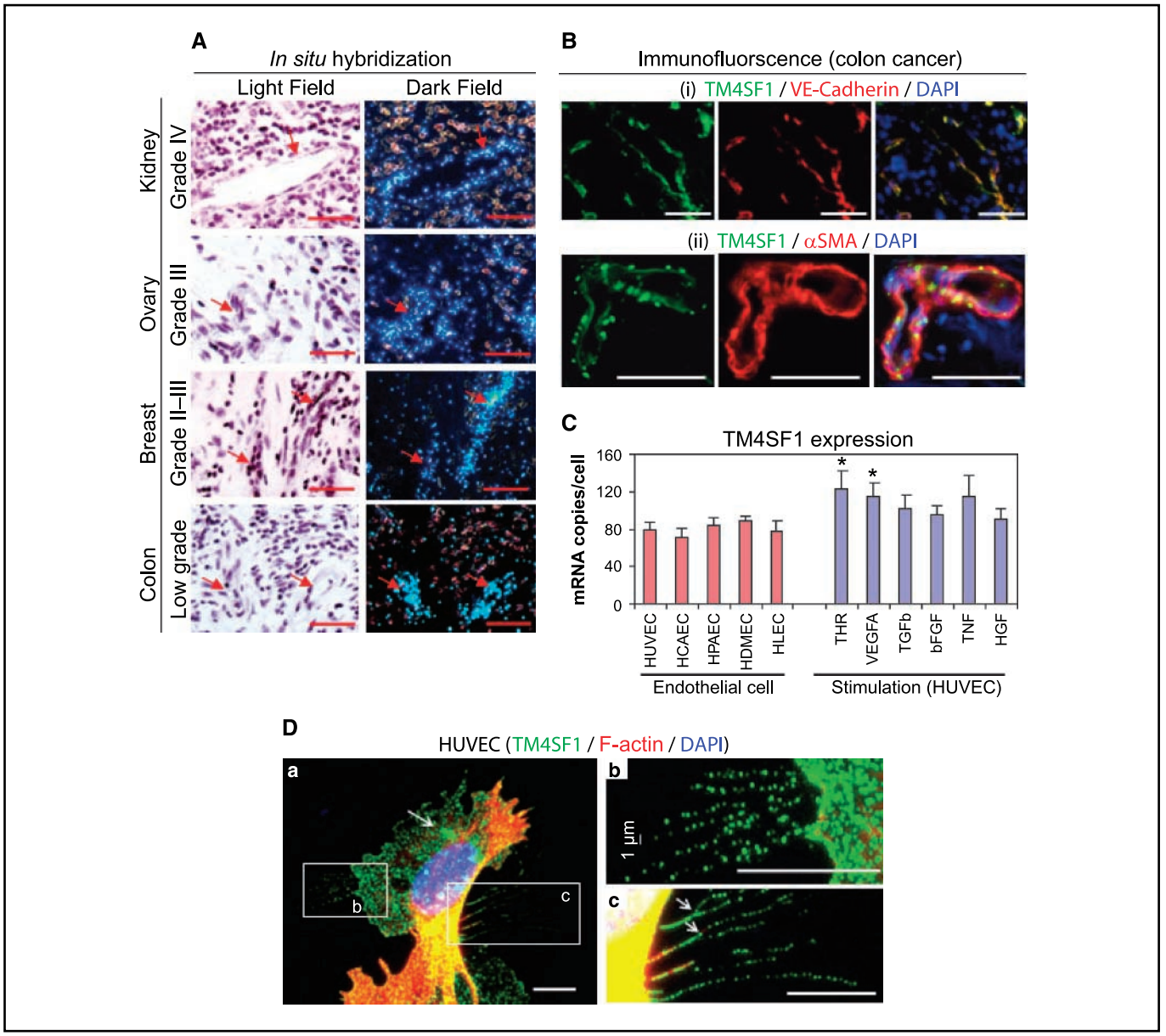

Figure 1. TM4SF1 expression in the vascular endothelium of human cancers and in cultured EC. *A, in situ* hybridization shows strong TM4SF1 expression in the blood vessels of colon, kidney, ovary, and breast carcinomas. Images shown are representative of those taken from four different patients with each type of cancer. Bright field reveals histology and dark field shows mRNA expression. *Arrows,* TM4SF1-positive blood vessels. *B,* immunofluorescence staining of a typical colon cancer with antibodies against TM4SF1 (*green*) and either (*i*) VE-cadherin or (*ii*) anti-human α-smooth muscle actin (*red*). *C,* TM4SF1 expression in several types of cultured EC (*left*) and in HUVEC stimulated with indicated growth factors (*right*). *, $P < 0.05$. *D,* TM4SF1 (*green*) and F-actin (*red*) double-staining of HUVEC reveals that TM4SF1 is localized to the plasma membrane, perinuclear vesicles (*arrow*), and particularly to filopodia (*a*). Filopodia exhibited a banded staining pattern (*b* and *c*). *Arrows,* filopodia branching (*c*). *Scale bars,* 100 μm (*A* and *B*) and 10 μm (*D*).

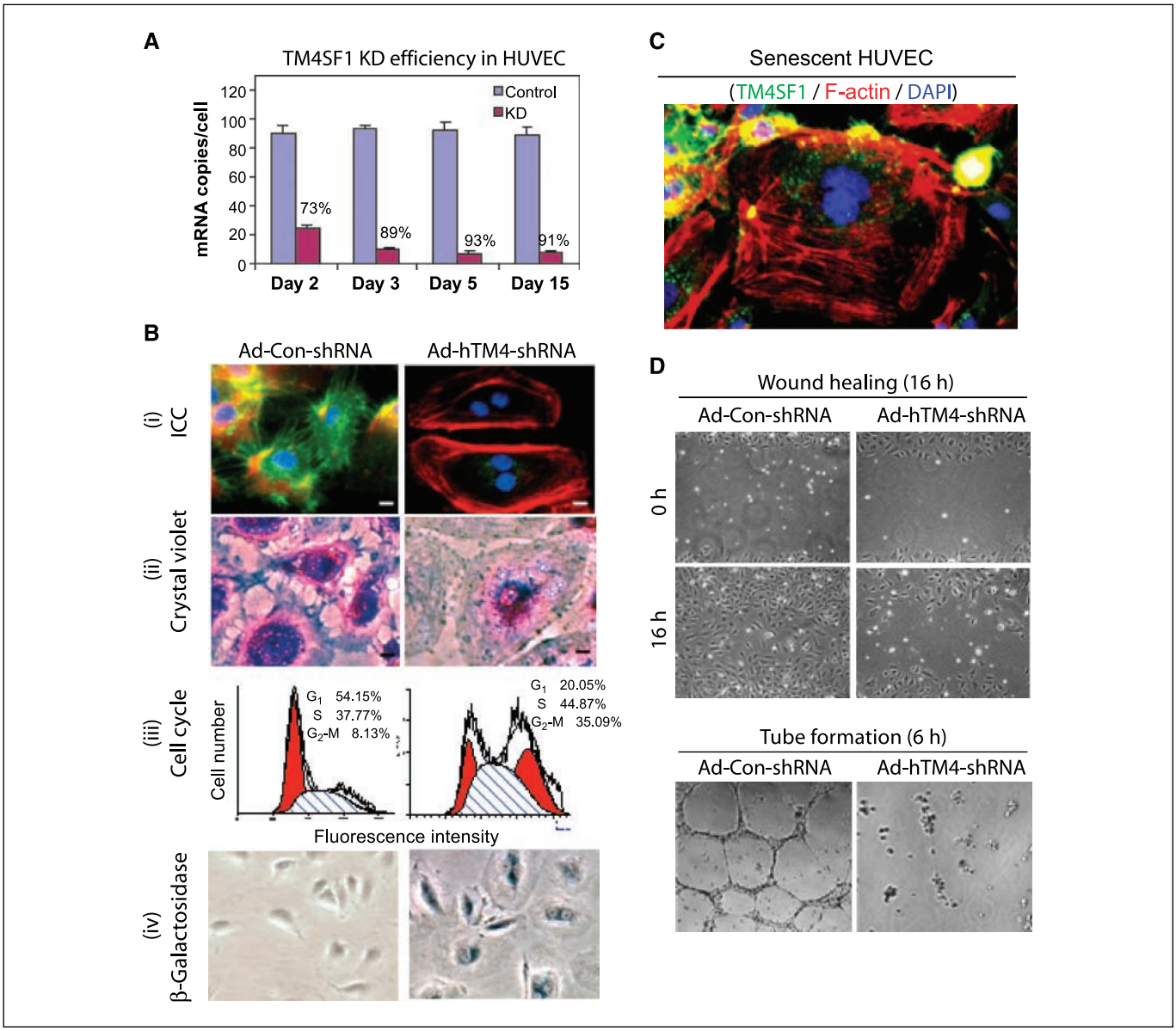

Figure 2. TM4SF1 KD rendered HUVEC senescent. *A,* TM4SF1 KD efficiency at various times after transfection with 50-moi Ad-hTM4-shRNA or Ad-Con-shRNA. *B,* day 3 TM4SF1-KD HUVEC lose TM4SF1 staining and develop stress fibers (*i*), lose filopodia (*i* and *ii*), increase cells in G_2-M by 4.3× (*iii*), and express β-galactosidase activity (*iv*). *C,* loss of TM4SF1 staining in a spontaneously senescent HUVEC. *D,* 3 d TM4SF1-KD HUVEC migrate poorly in a wound healing assay, fail to form tubes on Matrigel.

At 6 hours (but not at 1 or 18 hours), VEGF-A (20 ng/mL) and thrombin (1.5 units/mL) stimulated TM4SF1 expression modestly in HUVEC (~1.5-fold), whereas TGFβ (1 ng/mL), bFGF (50 ng/mL), TNFα (20 ng/mL), and HGF (20 ng/mL) did not significantly alter TM4SF1 expression at any time (Fig. 1*C, right*).

In subconfluent HUVEC, TM4SF1 was localized to the plasma membrane, to a minor population of perinuclear vesicles, and particularly to filopodia, some of which branched (Fig. 1*D*). Filopodia exhibited an intermittent, banded pattern of TM4SF1 staining (Fig. 1*Db* and *c*). F-actin, a quintessential filopodial marker, was confined to the most proximal portions of filopodia, generally within 10 μm of the cell body (Fig. 1*D*). Human coronary artery endothelial cell, human pulmonary artery endothelial cell, human dermal microvascular endothelial cell, and human lymphatic endothelial cell showed similar TM4SF1 staining patterns (data not shown). TM4SF1 was extracted by Triton X-100 concentrations >0.02%.

TM4SF1 knockdown in HUVEC. After transfection of HUVEC with either of two human TM4SF1 shRNAs, TM4SF1 mRNA abundance was reduced by 70% to 95% from days 2 to 15, whereas TM4SF1 expression was unaffected by control shRNA that does not recognize any known human or mouse mRNA (Fig. 2*A*).

TM4SF1 knockdown (KD) HUVEC underwent striking changes in structure and function. They enlarged greatly, accumulated numerous circumferential stress fibers, and were unable to complete cytokinesis, arresting in G_2-M (Fig. 2*Bi–iii*). Binucleate cells were observed a day after transfection, and by day 5, ~60% of cells were binucleate and 30% multinucleate. Nonetheless, KD cells remained viable for as long as they were followed in culture (15 days); throughout this period, 18S integrity was maintained and

Ki-67 expression levels were low (<10% of control cells) as determined by multigene transcriptional profiling. In addition, TM4SF1-KD HUVEC developed high levels of β-galactosidase activity (Fig. 2*Biv*), resisted trypsin detachment from culture dishes, and, once removed, reattached poorly. Furthermore, KD cells failed to migrate or proliferate after VEGF-A stimulation (data not shown). TM4SF1-KD HUVEC therefore exhibited senescence (17). Moreover, the occasional HUVEC that underwent spontaneous senescence in culture lost most of their TM4SF1 staining (Fig. 2*C*).

In addition, TM4SF1-KD HUVEC failed to extend filopodia (Fig. 2*Bi* and *ii*), migrated poorly in a wound healing assay, and failed to form tubes in Matrigel (Fig. 2*D*). Furthermore, although exhibiting extensive lamellipodial activity, KD HUVEC failed to move as much as a quarter cell diameter from their original position over 1.5 hours of time lapse imaging, whereas control shRNA-transfected HUVEC migrated extensively (Supplementary Fig. S1). TM4SF1 staining patterns and KD phenotype were similar in human pulmonary artery endothelial cell, human coronary artery endothelial cell, human dermal microvascular endothelial cell, and human lymphatic endothelial cell. However, cells that expressed TM4SF1 weakly (human dermal fibroblast, human smooth muscle cell) were unaffected by TM4SF1-KD (data not shown).

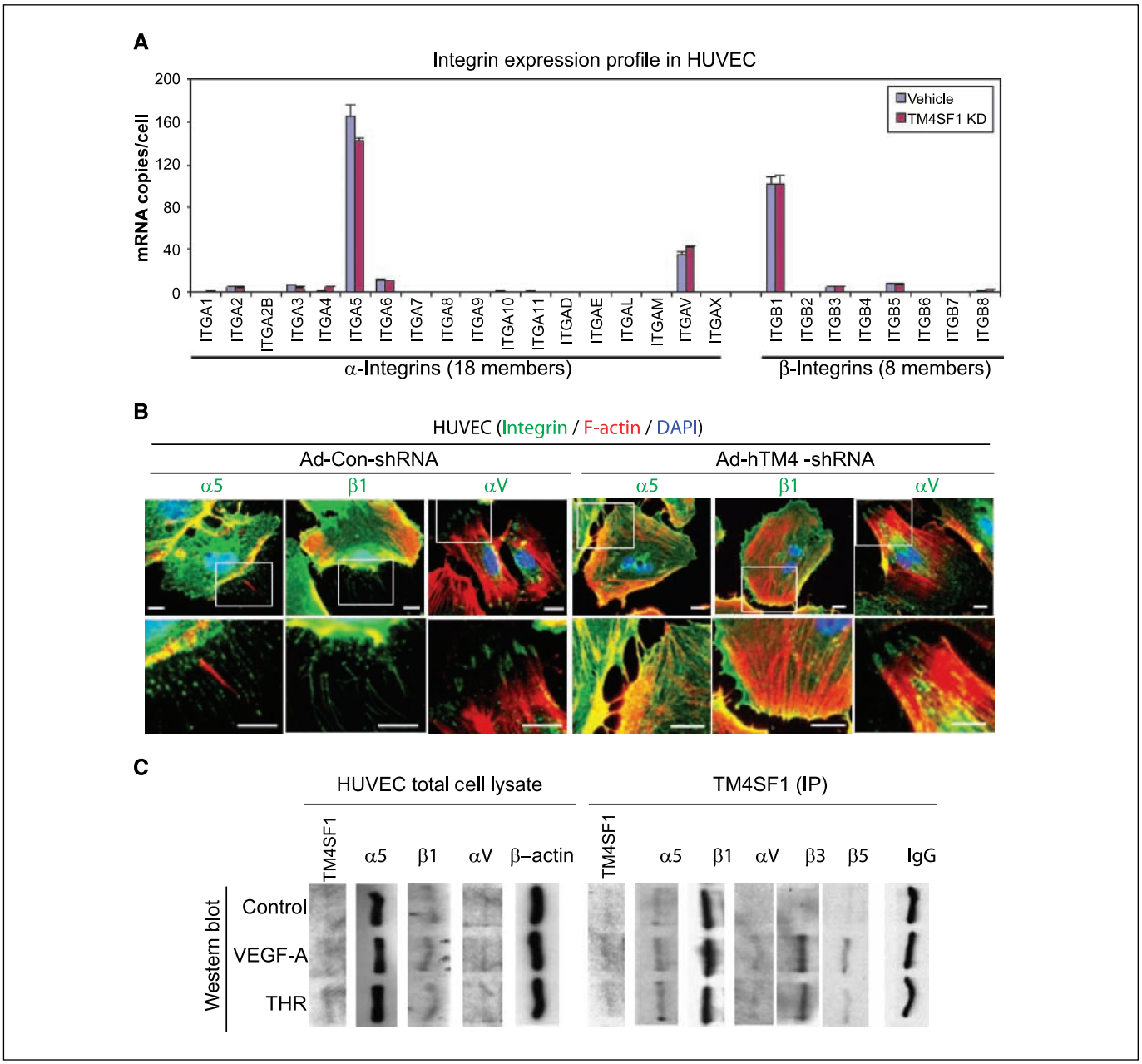

Figure 3. TM4SF1-integrin expression and interactions. *A,* integrin expression profile in HUVEC ± TM4SF1 KD. *B,* immunofluorescence staining of integrin α5, αV, and β1 subunits in HUVEC 3 d after 50-moi transfection with either Ad-hTM4-shRNA or Ad-Con-shRNA. *Scale bars,* 10 μm. *C,* control HUVEC or HUVEC stimulated for 6 h with VEGF-A (20 ng/mL) or thrombin (*THR*; 1.5 u/mL). Cell lysates, prepared before and after immunoprecipitation (*IP*) with anti-TM4SF1 antibody, were immunoblotted with indicated antibodies. IgG and β-actin were loading controls. The anti-TM4SF1 antibody effectively immunoprecipitated native TM4SF1 but reacted poorly with denatured TM4SF1. Expression of β3 and β5 were below detection levels in whole cell lysates.

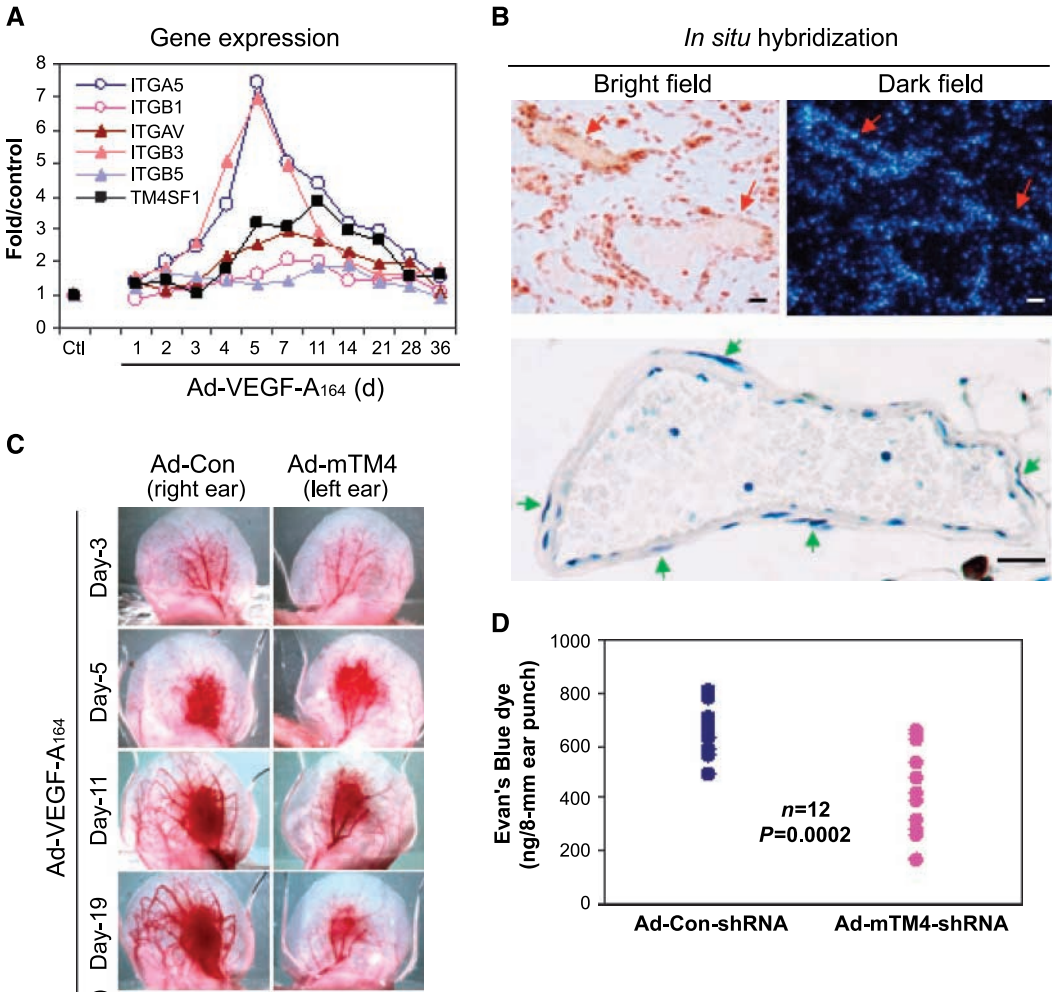

Figure 4. Expression of TM4SF1 and integrin subunits in Ad-VEGF-A^{164}–induced angiogenesis; effect of TM4SF1 on angiogenesis. *A,* mRNA expression levels of TM4SF1 and integrin subunits in mouse ears at indicated times after injection of 2.5 × 10^7 plaque-forming unit Ad-VEGF-A^{164}. *B, in situ* hybridization localization of TM4SF1 mRNA to VM in day 11 Ad-VEGF-A^{164}–injected mouse ears (*top*). Hematoxylin-stained VM illustrating smooth muscle cell coat (*green arrows, bottom*). *C,* angiogenic response in mouse ears at indicated times after Ad-VEGF-A^{164} injection. Moi (10^9) of Ad-mTM4-shRNA or Ad-Con-shRNA were injected into the right and left ears, respectively, 1 d before Ad-VEGF-A^{164} injection. The experiment was repeated four times. *D,* quantification of angiogenesis with the Evan's Blue dye 19 d after Ad-VEGF-A^{164} injection.

TM4SF1 interactions with integrins. Classic tetraspanins interact with integrins and participate in a variety of integrin-associated functions (18), but L6 family interactions with integrins have not been investigated. Of the 26 integrin subunits, only 3 (ITGA5, ITGAV, ITGB1) were highly expressed in HUVEC, and their expression was not affected significantly by TM4SF1-KD (Fig. 3*A*). Antibodies against α5 and -β1 stained filopodia in an intermittent, banded pattern (Fig. 3*B*), similar to that of TM4SF1 (Fig. 1*Db* and *c*). In contrast, αV staining was confined predominantly to focal contacts (Fig. 3*B*). Enlarged, binucleate TM4SF1-KD HUVEC continued to show normal α5, β1, and αV cell membrane staining (Fig. 3*B*). Thus, the failure of TM4SF1-KD HUVEC to form filopodia and migrate and is not attributable to changes in the abundances of α5, αV, or their β partners.

VEGF-A and thrombin are known to stimulate integrin expression and EC mobility (19, 20). These agents modestly but significantly increased ITGAV mRNA expression (1.4- to 1.6-fold) in HUVEC without affecting ITGA5 or ITGB1 expression (data not shown). Immunoblots revealed that both α5 and β1 associated constitutively with TM4SF1 and that these associations were minimally affected by VEGF-A or thrombin (Fig. 3*C*). However, interaction of TM4SF1 with αV and its β3 and β5 partners was only detected after VEGF-A or thrombin stimulation. Thus, TM4SF1, such as classic tetraspanins (18), interacts with integrins, and its pairing depends on the state of EC activation.

Role of TM4SF1 in VEGF-A–induced angiogenesis. To assess the role of TM4SF1 *in vivo*, we made use of an adenoviral vector expressing VEGF-A^{164} (Ad-VEGF-A^{164}) that induces an angiogenic

response in mouse tissues that closely mimics tumor angiogenesis (9, 10). Messenger RNA profiling showed that TM4SF1 expression increased at sites of Ad-VEGF-A^{164}–induced angiogenesis, although not in the initial (1–5 day) phase (Fig. 4*A*). This earliest phase of VEGF-A–induced angiogenesis is associated with the formation of mother vessels (MV), greatly enlarged, pericyte-poor sinusoids that derive from preexisting normal venules (11). Instead, TM4SF1 expression increased later, peaking at day 11 as MV differentiated into daughter vascular malformations (VM), MV that have acquired a smooth muscle cell coat (Fig. 4*B*). Expression of ITGAV, ITGB5, and ITGB1 mRNAs closely tracked that of TM4SF1, whereas ITGA5 and ITGB3 expression increased earlier with MV formation (Fig. 4*A*). Consistent with these findings, *in situ* hybridization showed that TM4SF1 was strongly expressed in VM (Fig. 4*B*).

We knocked down TM4SF1 by injecting an adenovirus expressing mouse TM4SF1–specific shRNA (Ad-mTM4-shRNA) into mouse ears 1 day before injection of Ad-VEGF-A^{164}. Ad-mTM4-shRNA did not affect the initial, MV phase of angiogenesis induced by Ad-VEGF-A^{164} (Fig. 4*C*). However, at day 11 and later, MV maturation into VM was substantially blunted by Ad-mTM4-shRNA but not by Ad-Con-shRNA (Fig. 4*C*). Vascular volume, a surrogate measure of angiogenesis, was significantly reduced in ears injected with Ad-mTM4-shRNA (Fig. 4*D*). VM formation was also reduced as determined by histology (data not shown). Thus, TM4SF1 plays a critical role in vessel maturation.

In summary, TM4SF1 is overexpressed in the blood vessels of several important human cancers. It is highly expressed in several types of cultured EC and is essential for their maintenance and function. When TM4SF1 was knocked down, HUVEC failed to form filopodia, became immobile, and assumed a senescent phenotype. Like classic tetraspanins, TM4SF1 interacts with integrins and may affect cell motility via such interactions. TM4SF1-KD affected vascular maturation in the Ad-VEGF-A^{164} mouse ear angiogenesis model, perhaps by interacting with integrins to mediate EC migration and promote cell-cell interactions. These data indicate that TM4SF1 is an important new player in EC biology that it could have potential in angiogenesis therapy.

Disclosure of Potential Conflicts of Interest

No potential conflicts of interest were disclosed.

Acknowledgments

Received 12/22/08; revised 2/24/09; accepted 3/3/09; published OnlineFirst 4/7/09.

Grant support: CLF Medical Technology Acceleration Program, Inc., Clifton, NY, by PO1 CA92644, and by NIH Shared Instrument Grant #:S10 RR017927.

The costs of publication of this article were defrayed in part by the payment of page charges. This article must therefore be hereby marked *advertisement* in accordance with 18 U.S.C. Section 1734 solely to indicate this fact.

References

1. Hellstrom I, Horn D, Linsley P, et al. Monoclonal mouse antibodies raised against human lung carcinoma. Cancer Res 1986;46:3917–23.
2. O'Donnell RT, DeNardo SJ, Shi XB, et al. L6 monoclonal antibody binds prostate cancer. Prostate 1998;37:91–7.
3. DeNardo SJ, O'Grady LF, Macey DJ, et al. Quantitative imaging of mouse l-6 monoclonal antibody in breast cancer patients to develop a therapeutic strategy. Int J Rad Appl Instrum B 1991;18:621–31.
4. Marken JS, Schieven GL, Hellstrom I, et al. Cloning and expression of the tumor-associated antigen l6. Proc Natl Acad Sci U S A 1992;89:3503–7.
5. Wright MD, Ni J, Rudy GB. The l6 membrane proteins-a new four-transmembrane superfamily. Protein Sci 2000;9:1594–600.
6. Chang YW, Chen SC, Cheng EC, et al. Cd13 (aminopeptidase n) can associate with tumor-associated antigen l6 and enhance the motility of human lung cancer cells. Int J Cancer 2005;116:243–52.
7. Lekishvili T, Fromm E, Mujoomdar M, et al. The tumour-associated antigen l6 (l6-ag) is recruited to the tetraspanin-enriched microdomains: Implication for tumour cell motility. J Cell Sci 2008;121:685–94.
8. Kao YR, Shih JY, Wen WC, et al. Tumor-associated antigen l6 and the invasion of human lung cancer cells. Clin Cancer Res 2003;9:2807–16.
9. Pettersson A, Nagy JA, Brown LF, et al. Heterogeneity of the angiogenic response induced in different normal adult tissues by vascular permeability factor/vascular endothelial growth factor. Lab Invest 2000;80:99–115.
10. Nagy JA, Shih SC, Wong WH, et al. Chapter 3. The adenoviral vector angiogenesis/lymphangiogenesis assay. Methods Enzymol 2008;444:43–64.
11. Nagy JA, Dvorak AM, Dvorak HF. Vegf-a and the induction of pathological angiogenesis. Annu Rev Pathol 2007;2:251–75.
12. Brown LF, Dezube BJ, Tognazzi K, et al. Expression of tie1, tie2, and angiopoietins 1, 2, and 4 in kaposi's sarcoma and cutaneous angiosarcoma. Am J Pathol 2000;156:2179–83.
13. Sundberg C, Nagy JA, Brown LF, et al. Glomeruloid microvascular proliferation follows adenoviral vascular permeability factor/vascular endothelial growth factor-164 gene delivery. Am J Pathol 2001;158:1145–60.
14. Shih SC, Smith LE. Quantitative multi-gene transcriptional profiling using real-time pcr with a master template. Exp Mol Pathol 2005;79:14–22.
15. Aerts JL, Gonzales MI, Topalian SL. Selection of appropriate control genes to assess expression of tumor antigens using real-time rt-pcr. Biotechniques 2004;36:84–6.
16. Hollenhorst PC, Jones DA, Graves BJ. Expression profiles frame the promoter specificity dilemma of the ets family of transcription factors. Nucleic Acids Res 2004;32:5693–702.
17. Kurz DJ, Decary S, Hong Y, et al. Senescence-associated (β)-galactosidase reflects an increase in lysosomal mass during replicative ageing of human endothelial cells. J Cell Sci 2000;113:3613–22.
18. Hemler ME. Tetraspanin functions and associated microdomains. Nat Rev Mol Cell Biol 2005;6:801–11.
19. Senger DR. Molecular framework for angiogenesis: A complex web of interactions between extravasated plasma proteins and endothelial cell proteins induced by angiogenic cytokines. Am J Pathol 1996;149:1–7.
20. Maragoudakis ME, Tsopanoglou NE, Andriopoulou P. Mechanism of thrombin-induced angiogenesis. Biochem Soc Trans 2002;30:173–7.